A BLACK-BOX BACK-PROJECTION ALGORITHM FOR ELECTRICAL IMPEDANCE TOMOGRAPHY

Pai, Chi Nan
Department of Mechatronic and Mechanical Systems Engineering - Polytechnic School of University of São Paulo Av. Prof. Mello de Moraes, 2231 - São Paulo - SP - 05508-900, Brazil
pai.nan@poli.usp.br

Moura, Fernando Silva de
Department of Mechanical Engineering - Polytechnic School of University of São Paulo Av. Prof. Mello de Moraes, 2231 - São Paulo - SP - 05508-900, Brazil
fernando.moura@poli.usp.br

Schweder, Ronaldo K.
Department of Mechanical Engineering - Polytechnic School of University of São Paulo Av. Prof. Mello de Moraes, 2231 - São Paulo - SP - 05508-900, Brazil
ronaldo.schweder@poli.usp.br

Mirandola, Luis A. S.
Department of Mechatronic and Mechanical Systems Engineering - Polytechnic School of University of São Paulo Av. Prof. Mello de Moraes, 2231 - São Paulo - SP - 05508-900, Brazil
luis.mirandola@poli.usp.br

Aya, Julio C. C.
Department of Mechanical Engineering - Polytechnic School of University of São Paulo Av. Prof. Mello de Moraes, 2231 - São Paulo - SP - 05508-900, Brazil
jccaya@usp.br

Lima, Raul Gonzalez
Department of Mechanical Engineering - Polytechnic School of University of São Paulo Av. Prof. Mello de Moraes, 2231 - São Paulo - SP - 05508-900, Brazil
rauglima@usp.br

Abstract. *Electrical Impedance Tomography (EIT) estimates resistivity distribution based on measurements of electrical potential on the boundaries of a domain of interest. One of the applications is to monitor the lung of patients under Intensive Care Treatment, for instance, for adjusting a ventilator. The well known back-projection algorithm for EIT has low spatial resolution and non uniform sensitivity. The present work investigates the possibility of identifying directly the back-projection matrix given known perturbations of the resistivity distribution and their associated boundary electrical potential perturbations. The boundary electrical potential perturbations were obtained from numerical simulations and through experimental data. The numerical simulations use tri-dimensional Finite Element model and electrodes model. The black-box back-projection matrix is estimated minimizing an error index. The performance of the black-box back-projection matrix is addressed comparing with the back-projection algorithm described by Santosa and Vogelius 1990. The blur-radius of an object on a saline medium is computed for both algorithms and different positions of the object. The new algorithm proposed has the structure of the back-projection algorithm, as described by Santosa and Vogelius, with flexibility for incorporating correct geometry, 3D finite element mesh, complete electrode model, and a priori information.*

Keywords: *back-projection, black-box, Electrical Impedance Tomography, phantom*

1. Introduction

Electrical Impedance Tomography (EIT) is a method of imaging the resistivity distribution within a volume. The images are reconstructed from a set of electrical potential measurements on the boundaries of a domain of interest, which is a section of this volume. These electrical potentials can be obtained by applying current between two adjacent electrodes and measuring the resulting voltage profile between all other adjacent electrodes around the boundary of interest. At present day, there are several different reconstruction algorithms, such as: Newton-Raphson, Sensitivity method, Perturbation method, Equipotential lines, Iterative equipotential lines, double constraint (Yorkey and Webster, 1986). The equipotential lines method, also known as back-projection algorithm (Barber and Brown, 1984), is exceptional in achieving a moderate accuracy at an extremely low computational cost, but it has a poor spatial resolution and non uniform

sensitivity, due to the smoothness of the base of functions used to form an image. Besides, since each transfer impedance (ratio of potential to the applied current) is the result of a volume integral, and it is affected by the body shape (Brown, 2003), many of these algorithms, including back-projection, use difference imaging. In the present paper, these problems are solved by using a tri-dimensional finite elements method with electrode model, and, by identifying directly the back-projection matrix given known perturbations of the resistivity distribution and their associated boundary electrical potential perturbations, the effect of limited number of potential measurements is attenuated, improving the spatial resolution.

2. Numerical Phantom

The numerical phantom algorithm simulates an actual EIT tomograph. It obtains all the electrical potentials on the boundary of domain for each current injection pattern in this domain, with known electrical resistivity distribution. Since this distribution can be chosen, it is possible to simulate the existence of one or more regions with smooth shape and resistivity. The method performs better if the domain have the same geometry and size of the model used for reconstruction and, since the data is generated through an experimental setup, there is no *inversion crime*.

The Phantom implementation uses the finite elements model for domain discretization and assumes that each element has constant resistivity. The determination of electrical potentials on the domain is called the direct or forward problem, given the cause (resistivity distribution and current pattern) search the effect (electrical potentials).

The finite element direct problem is represented by

$$\mathbf{Y}|_{\rho} U = c \tag{1}$$

where $\mathbf{Y}$ is the conductivity matrix of the system, c is the vector of currents and U is the vector of nodal electrical potentials.

For each current injection pattern, this linear system is solved for the electrical potentials at the electrodes and used to estimate the black-box back-projection matrix.

2.1 A 3D Model of the skin/electrode interface

For the present paper, a tri-dimensional electrode interface model was developed based on the 2D model proposed by Hua *et al.* (1993). This model considers that each interface is composed by two neighbour hexahedrons. After the development of the conductivity matrix, the columns and the lines of nodes which represent the electrode surface are added, because the electrical potential at each node are supposed to be the same. Besides, it is assumed that the interface resistivity is isotropic. Figure 1 shows some of the dimensions of the interface and the node numbering sequence.

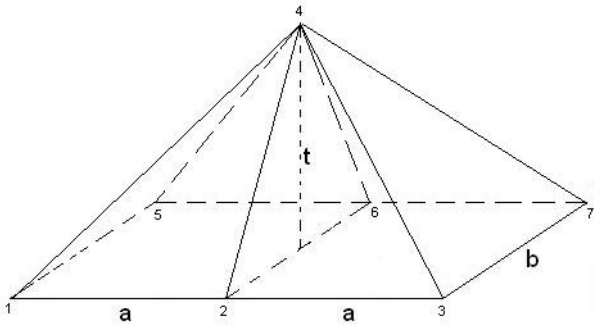

Figure 1. Interface Model

The conductivity matrix of the interface results,

$$[Y_{el}] = \frac{ab}{9\rho t}\begin{bmatrix} 1 & \frac{1}{2} & 0 & -\frac{9}{4} & \frac{1}{2} & \frac{1}{4} & 0 \\ & 2 & \frac{1}{2} & -\frac{9}{2} & \frac{1}{4} & 1 & \frac{1}{4} \\ & & 1 & -\frac{9}{4} & 0 & \frac{1}{4} & \frac{1}{2} \\ & & & 18 & -\frac{9}{4} & -\frac{9}{2} & -\frac{9}{4} \\ & & & & 1 & \frac{1}{2} & 0 \\ & S & Y & M & & 2 & \frac{1}{2} \\ & & & & & & 1 \end{bmatrix}, \tag{2}$$

where the node 4 is the one which represents the outer surface of the electrode, and the others form the skin/electrode surface and a, b and t represent the dimensions of the interface.

3. Back-Projection

The back-projection algorithm, as described by Santosa and Vogelius (1990), uses the electrical potential measurements of a certain domain to estimate the resistivity distribution inside this domain. Its mathematical model is:

$$\frac{\Delta\rho_i}{\rho_i^0} = \frac{1}{m}\sum_{j=1}^{m}\frac{\partial U_j}{U_j^0}W_{i,j}, \tag{3}$$

where $\frac{\Delta\rho_i}{\rho_i^0}$ is the resistivity perturbation in the i-*th* pixel of the domain, m is the number of electrodes, ∂U_j is the variation in the electrical potential of the j-*th* electrode, U_j^0 is the electrical potential at the j-*th* electrode corresponding to the initial resistivity distribution ρ_i^0, and $W_{i,j}$ are the back-projection weight parameters.

In matrix form, eq. 3 results

$$\left[\frac{\Delta\rho}{\rho^0}\right] = [B]\left[\frac{\Delta U}{U^0}\right], \tag{4}$$

where $\left[\frac{\Delta\rho}{\rho^0}\right]$ is the normalized resistivity distribution vector of the domain, $\left[\frac{\Delta U}{U^0}\right]$ is the electrode normalized electrical potential measurements vector and $[B]$ is the back-projection matrix.

4. Black-Box

The main idea of the black-box back-projection method is that if good images, relative variations of resistivity, and good measurements, relative variations of electrode potentials, are available, then a matrix that relate measurements and images may be estimated. The method forms a set of difference images and computes, using a finite element model, the respective variations on electrode potentials. From these two sets of information it estimates the back-projection matrix.

The black-box back-projection algorithm estimates directly the $\mathbf{B}$ matrix of back-projection given the variation of potential on the boundary of the domain when the resistivity of each finite element of domain varies. The method assumes linearity between variation of potentials at the electrodes and variation of electrical resistivity.

First, it is assumed an initial resistivity distribution which will be used as reference. With this reference, the electrical potentials are calculated, using a Finite Element model, for each current injection pattern. A perturbation is imposed on each finite element, one at a time. The potentials at the electrodes are calculated and normalized with respect to the potential corresponding to the reference value. The perturbed potentials are arranged as vectors. A matrix of perturbed potentials is formed such that each column of this matrix is a perturbed potential vector. Through the perturbed potential matrix and a matrix of resistivity perturbation, the matrix $\mathbf{B}$ can be determined.

The procedure to determine $\mathbf{B}$ is:

1. assume a known electrical resistivity at each one of n elements of domain, arrange as vector ρ^0. The linearization of the model is performed around ρ^0.

2. each current injection pattern is denoted by $\{c_j\}_{m\times 1}$ for $j = 1, 2, \ldots, m$;

3. the potentials at the electrodes, U_j^0, are determined from the direct problem,

$$\mathbf{Y}|_{\rho^0} U_j^0 = c_j \qquad , \qquad j = 1, 2, \ldots, m. \tag{5}$$

4. a known perturbation on the resistivity element of the i-*th* element of ρ^0, is denoted by $\delta\rho_i$ and $i = 1, 2, \ldots, n$;

5. vectors $\{\delta\rho^i\}_{n\times 1}$ are formed such that all elements are null but the i-*th* element that contains $\delta\rho_i$, i. e., $\delta\rho^i = \delta\rho_i$;

6. for each current pattern c_j, the potentials at electrodes, $\{U_j^i\}$ related to a resistivity perturbation $\delta\rho^i$ are determined by the direct problem,

$$\mathbf{Y}|_{(\rho^0+\delta\rho^i)} U_j^i = c_j \qquad , \qquad j = 1, 2, \ldots, m \qquad , \qquad i = 1, 2, \ldots, n. \tag{6}$$

7. let $\{U^0\}_{m^2\times 1}$ be an augmented vector formed of $\{U_j^0\}_{m\times 1}$ for $j = 1, 2, \ldots, m$, such that,

$$U^0 = \begin{bmatrix} U_1^0 \\ U_2^0 \\ \cdots \\ U_m^0 \end{bmatrix} \tag{7}$$

8. let $\{U^i\}_{m^2\times 1}$ be an augmented vector formed of $\{U_j^i\}_{m\times 1}$ for $j = 1, 2, \ldots, m$, such that

$$U^i = \begin{bmatrix} U_1^i \\ U_2^i \\ \cdots \\ U_m^i \end{bmatrix} \tag{8}$$

9. form a normalized vector $\{\psi^i\}_{n\times 1}$ such that each element, for $j = 1, 2, \ldots, n$, is

$$\{\psi^i\}_j = \frac{\delta\rho^i{}_j}{\rho_j^0} \tag{9}$$

10. form a normalized vector $\{\theta^i\}_{m^2\times 1}$ such that each element, for $j = 1, 2, \ldots, n$, is

$$\{\theta^i\}_j = \frac{U^i - U^0{}_j}{U^0{}_j}, \tag{10}$$

11. define a matrix $\mathbf{\Psi}_{n\times n}$ such that

$$\mathbf{\Psi}_{n\times n} = \begin{bmatrix} \psi^1 & \ldots & \psi^i & \ldots & \psi^n \end{bmatrix}, \tag{11}$$

observe that this matrix is diagonal;

12. define a matrix $\mathbf{\Theta}_{m^2\times n}$ such that

$$\mathbf{\Theta}_{m^2\times n} = \begin{bmatrix} \theta^1 & \ldots & \theta^i & \ldots & \theta^n \end{bmatrix} \tag{12}$$

13. since each column of Ψ is an image and can be related to a column of Θ by a back-projection matrix, one can say,

$$\mathbf{\Psi}_{n\times n} = \mathbf{B}_{n\times m^2} \mathbf{\Theta}_{m^2\times n} \tag{13}$$

14. finally, determine the matrix $\mathbf{B}$ that minimizes an error index, eq. 18.

Once the matrix $\mathbf{B}$ is obtained, estimation of a difference image is performed multiplying B and a normalized vector of variation of electrode potentials related to each current injection pattern, according to eq. 14

$$\Delta\rho = \mathbf{B}\Delta U \tag{14}$$

where $\{\Delta\rho\}_{n\times 1}$ is such that the i-*th* element is $\frac{\rho-\rho^0{}_i}{\rho^0{}_i}$ for $i = 1, 2, \ldots, n$, and $\{\Delta U\}_{n^2\times 1}$ is such that the j-*th* element is $\frac{U_{measured}-U^0_{measured_j}}{U^0_{measured_j}}$ for $j = 1, 2, \ldots, m^2$.

4.1 Determination of B

The matrix $\mathbf{\Theta}^T\mathbf{\Theta}$ is ill-conditioned, so its inversion for $\mathbf{B}$ determination introduce great numerical errors. Therefore, to determine $\mathbf{B}$, a regularization is necessary.

An error index is defined as,

$$IE = tr\left\{\mathbf{E}^T\mathbf{E} + \alpha\mathbf{B}^T\mathbf{F}^T\mathbf{F}\mathbf{B} + \beta\mathbf{B}^T\mathbf{M}^T\mathbf{M}\mathbf{B}\right\}, \tag{15}$$

where $\mathbf{F}$ is a high pass spatial filter considering a column of $\mathbf{B}$ like an image, $\mathbf{M}$ is an uniform sensitivity matrix, α and β are regularizations parameters, and matrix $\mathbf{E}$ is defined as

$$\mathbf{E} = \mathbf{\Theta}(\mathbf{\Psi} - \mathbf{B}\mathbf{\Theta}). \tag{16}$$

The matrix $\mathbf{M}$ is a diagonal matrix such that on each element of the diagonal there is a number computed by eq. 17

$$M_{ii} = r(i)^p, \tag{17}$$

where $r(i)$ is the distance of the geometrical center of the i-*th* finite element to the center of the container, divided by the radius of the container. And p is a experimentally adjusted real parameter, to attenuate localization error and non-uniform sensitivity.

The minimum of the error index with respect to $\mathbf{B}$ is achieved when,

$$\mathbf{B} = (\mathbf{\Theta}^T\mathbf{\Theta} + \alpha\mathbf{F}^T\mathbf{F} + \beta\mathbf{M}^T\mathbf{M})^{-1}\mathbf{\Psi}\mathbf{\Theta}^T. \tag{18}$$

5. Parameters and methodology

The mesh used to create the matrix $\mathbf{B}$ has 300.0 mm of diameter, $n = 2034$ pentahedrical elements (prisms of triangular base), divided equally in three layers, 30.0 mm of total height and $e = 30$ electrodes. The Fig. 2 shows the top view of the mesh.

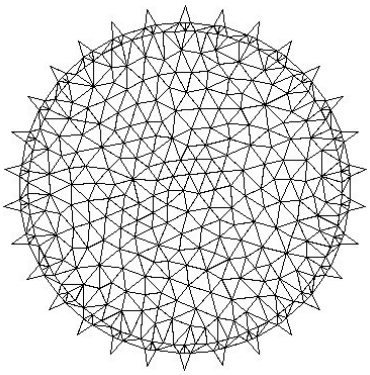

Figure 2. Finite Element Mesh

Figure 3. Experimental Container

The initial distribution of electrical resistivity $\{\rho^0\}$ was homogeneous and equal to $3.0\,\Omega m$. The electrodes parameters were all equal to $0.02\,\Omega m^2$. The imposed perturbation $\delta\rho^i$ was $+30\%$ of initial value.

The electrical potential data set was collected from an experimental cylindrical container shown on Fig. 3 filled with 0.5% saline solution. An acrylic cylinder with 32 mm of diameter was used to simulate a region with different electrical resistivity. The object will be analyzed on two positions. Position 1 has the object placed at the center of the container. Position 2 has the object placed 120 mm apart from the center of the container.

Since the spatial resolution and sensitivity of EIT is dependent on the radial position. The blur radius is used frequently to evaluate the spatial resolution, Adler (1995). The blur radius will be used to compare both algorithms.

The blur radius (BR) is a measure of spatial resolution. It is defined by

$$\mathbf{BR} = \frac{r_z}{r_0} = \sqrt{\frac{A_z}{A_0}}, \tag{19}$$

where A_z is the area of the plane that divides the volume under a 3D plot of the image by 2, and A_0 is the area of the container.

The methodology of the tests consists on determining the blur radius obtained using the back-projection algorithm and the black-box algorithm. Since the black-box algorithm has two regularization parameters α and β, the blur radius values were computed varying the values of these parameters from 1.0 e-12 to 1.0 e-1, to help he choice of the regularization parameters.

6. Analysis of the Black-Box regularization parameters

To determine the value of the regularization parameters (α, β), the following index, based on the blur-radius concept, was defined as

$$\Gamma = \frac{BR}{\frac{r}{r_o}}, \tag{20}$$

where BR is the blur-radius, r is the radius of cylinder and r_o is the radius of the container. This index Γ represents the ratio between the blur radius from the image and the blur radius of the real cylinder. The Fig.4(a) and Fig. 4(b) show the values of Γ for each pair (α, β) at both positions.

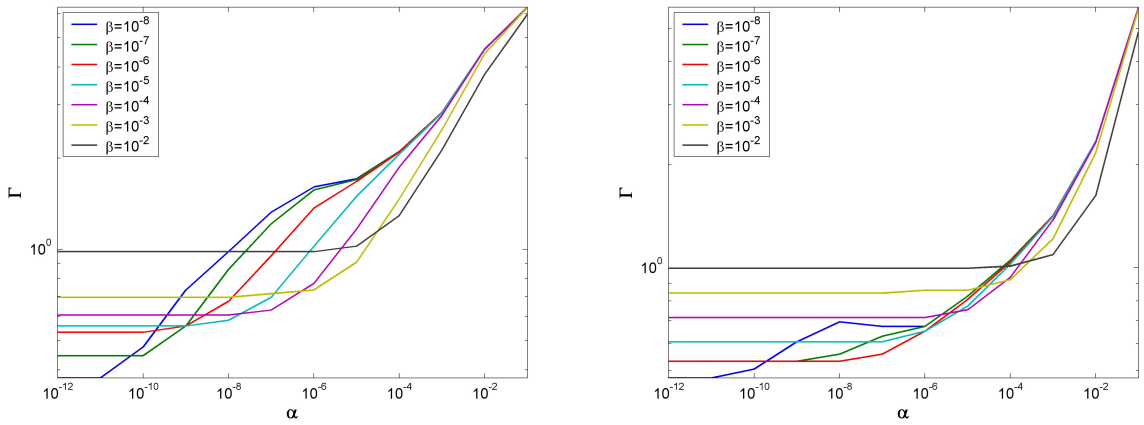

(a) Cylinder at position 1

(b) Cylinder at position 2

Figure 4. L-curves using index Γ

In this paper, it was used $\alpha = 1.0$ e-4 and $\beta = 4.0$ e-3. The value of β was chosen to give uniform sensitivity on the domain, i.e., approximately the same diameter and amplitude of the acrylic object on the image, no matter the position of the object. The value of α was chosen from the L-curves shown on Fig. 4(a) and Fig. 4(b) where $\beta = 4.0$ e-3. We take a value of α close to the corner of the L-curves.

7. Results

Four images resulting from experimental data are presented. The first two images were obtained through the back-projection algorithm as described by Santosa and Vogelius (1990). The image on Fig. 5 represents the phantom with an acrylic object at position 1. The image on Fig. 6 represents the phantom with an acrylic object at position 2.

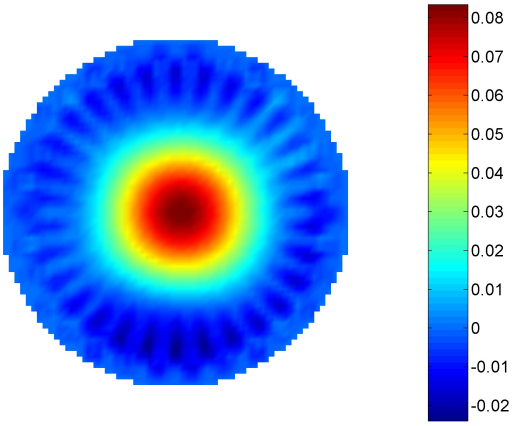

Figure 5. Center of the object 0.0 mm apart from center, Back-Projection, BR $= 0.23$

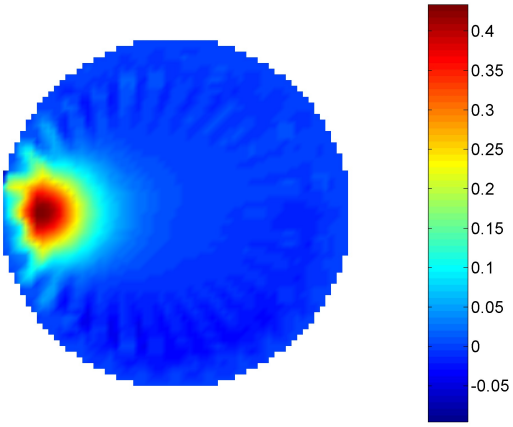

Figure 6. Center of the object 120.0 mm apart from center, Back-Projection, BR $= 0.16$

The following images result from the same experimental data and using the black-box back-projection algorithm. The image on Fig. 7 represents the phantom with an acrylic object at position 1. The image on Fig. 8 represents the phantom with an acrylic object at position 2.

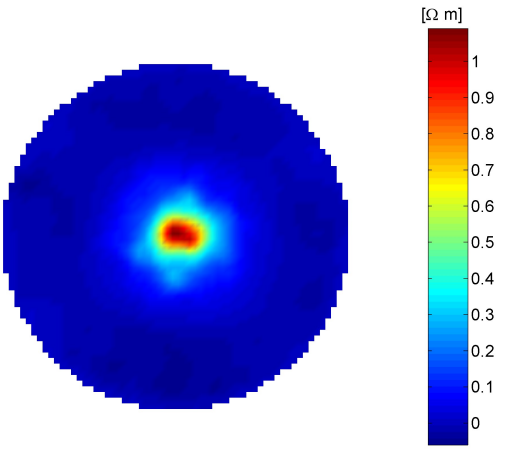

Figure 7. Center of the object 0.0 mm apart from center, Black-Box Back-Projection, BR $= 0.14$

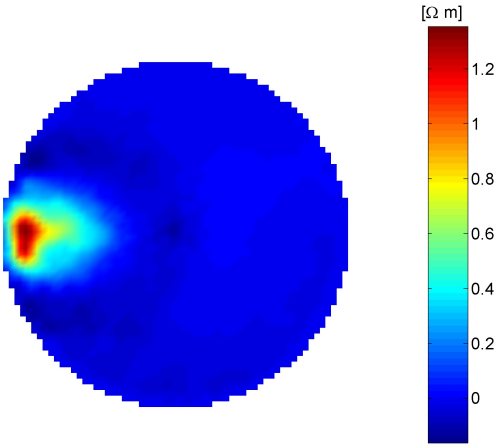

Figure 8. Center of the object 120.0 mm apart from center, Black-Box Back-Projection, BR $= 0.10$

8. Discussion

From Fig. 5 and Fig. 6 the amplitude of the acrylic cylinder diminished 81.4% when it was moved from position 2 to position 1. From Fig. 7 and Fig. 8 the amplitude of the acrylic cylinder diminished only 18.5% when it was moved from position 2 to position 1. It suggests that the sensitivity of the black-box back-projection is more uniform.

The Blur-Radius obtained from images generated by the back-projection algorithm, specifically BR $= 0.23$ and BR $= 0.16$ for positions 1 and 2, respectively, are larger than the Blur-Radius obtained from images generated by the black-box back-projection,specifically BR $= 0.14$ and BR $= 0.10$ for positions 1 and 2, respectively. It suggests that the spatial resolution of the black-box back-projection is better than the back-projection described by Santosa and Vogelius.

9. Conclusion

A new difference image algorithm was proposed with flexibility for incorporating correct geometry, 3D finite element mesh, complete electrode model, and a priori information. It has the structure of the back-projection algorithm, as described by Santosa and Vogelius, in its last matrix multiplication. Furthermore, through our preliminary results the spatial resolution and uniformity of sensitivity seem improved.

10. Acknowledgements

Financial Supports by The State of Sao Paulo Research Foundation, process 01/05303-4 is gratefully acknowledged.

11. References

Adler, A.,1995, "Measurement of Pulmonary Function with Electrical Impedance Tomography", Ph.D., Université de Montréal.

Barber, D.C. and Brown, B.H.,1984, "Applied Potential Tomography", Journal of Physics E: Scientific Instruments, vol.17, No. 9, pp.723 - 733.

Brown, B.H.,2003, "Electrical impedance tomography (EIT): A review", Journal of Medical Engineering and Technology, vol.27, No. 3, pp.97 - 108.

Hua, P., Woo, E.J., Webster, J.G. and Tompkins, W.J.,1993, "Finite element modeling of electrode-skin contact impedance in electrical impedance tomography", IEEE Transactions on Biomedical Engineering, vol.40, No. 4, pp.335 - 343.

Santosa, F. and Vogelius, M.,1990, "Backprojection algorithm for electrical impedance imaging", SIAM Journal on Applied Mathematics, vol.50, No. 1, pp.216 - 243.

Yorkey, T.J. and Webster, J.G.,1986, "Comparison Of Impedance Tomographic Reconstruction Algorithms", Clinical Physics and Physiological Measurement, vol.8 supp A, pp.55 - 62.

12. Responsibility notice

The authors are the only responsible for the printed material included in this paper